Title
ENHANCED RECOVERY WITH MOBILITY AND REACTIVE TENSION AGENTS.

Authors
Radke, CJ
Somerton, WH

Publication Date
1976

Peer reviewed

Oil & Gas J., DOE Symp., 1A-Oil, p. B-2/1-27 (1978).

ENHANCED RECOVERY WITH MOBILITY AND REACTIVE TENSION AGENTS

by

C. J. Radke and W. H. Somerton
Lawrence Berkeley Laboratory and Departments
of Chemical and Mechanical Engineering
University of California
Berkeley, California 94720

ABSTRACT

To establish and improve recovery efficiencies of acidic crude oils with alkaline agents this project includes studies on displacement dynamics, interfacial tensions, emulsion flow and caustic loss. Displacement tests on restored Wilmington oil-field cores with caustic under anticipated field operating conditions show recoveries of about 30% of the oil remaining after water-flooding and caustic loss to the reservoir sand. Displacement results for synthetic systems show 50% tertiary recovery efficiencies under specific tailoring of pH and ionic strength. Concomitant experiments with interfacial tensions, contact angles, and emulsion type and stability demonstrate the importance of wettability alteration. Dynamic spinning-drop interfacial tensions of Wilmington crude oils show deep minima whose depth and attainment time are strong functions of pH and salt content. A mass transfer model, based on the concept of sorption barriers, correctly reflects these time-evolving tensions and permits extrapolation of the spinning-drop data to field conditions. An emulsion flow model based on filtration theory has been devised and numerically solved to predict correctly permeability behavior. Caustic adsorption loss on Ranger-zone Wilmington reservoir sand, determined by frontal-analysis chromatography, is critically dependent on pH.

INTRODUCTION

Use of alkaline solutions to recover selected acid crude oils has considerable economic advantage over commercial surfactant solutions. In spite of the longevity of the idea, however, considerable question remains as to its displacement effectiveness (1). The objectives of the present study are (1) to establish the conditions requisite for tertiary-mode displacement of acidic oils with high pH agents, and (2) to elucidate the dominant recovery mechanisms and hence permit development of an improved caustic flooding package. The overall project includes studies on core displacements from synthetic and natural systems, interfacial tensions, emulsion rheology and stability in porous media, and caustic loss. A summary of our progress in these areas

Prepared for the Department of Energy under Contract No. W-7405-ENG-48

since the 1977 report (2) follows.

CORE DISPLACEMENTS

Oil Field Studies

Caustic flooding tests have been run at reservoir temperature on a number of Ranger-zone cores using Ranger crude oil and simulated formation water. The test apparatus is similar to that used previously (2) except that the core is mounted in a water bath maintained at a constant temperature of 125 ± 1°F. During saturation of the cores with Ranger-zone crude, the temperature of the system is increased to 180°F to ensure that all the asphaltenes are in solution in the crude since these constituents may play an important role in the crude oil behavior. This high temperature has led to failure of several types of plastic core holders which have been used to minimize the corrosive effects of the caustic solutions. Currently, a thick-walled Teflon tube is used as the core holder with moderate success.

Frozen Ranger-zone cores are diamond drilled using liquid nitrogen and then are quickly packed into the Teflon core holder under moderate pressure. The packed core is then mounted in the system and slowly brought to reservoir temperature. In the first series of tests, the native state cores were first water-flooded with 1.43% NaCl brine. In all cases, the oil saturation was too low to recover oil (see Table 1). The water flood was then followed by a caustic flood (0.1 wt% NaOH in softened Colorado River water followed by 0.1% NaOH plus 1.0% NaCl in the same water)at a 1.5 ft/day rate. Again the oil saturation was too low to recover oil

The native state cores were extracted in-situ using toluene followed by an acetone wash. (Since acetone was contributing to failure of the plastic tubes, the cleaning procedure was later changed to use Chevron 410H solvent followed by isopropyl alcohol), After extracting and drying, the cores were saturated with brine and the brine was displaced with crude oil to irreducible water saturation. The water flooding and caustic flooding procedures were as given above, following THUMS planned procedure for field tests (3).

Results of several of the tests are summarized in Table 1. The earlier test cores (A and B) had high porosities and permeabilities. By improved packing techniques in later cores (C), the porosity and permeability were greatly reduced. The resaturated core A-2 recovered 46% of the oil in place by water flood and an additional 20% by caustic flood for a total recovery efficiency of 66%. The second resaturated core gave much lower recovery efficiencies: 27% by water flood and an additional 10% by caustic. The large difference in the behavior of these two similar cores can probably be attributed to the lower initial oil saturation in the latter case.

Test core C-1 was prepared by a modified packing procedure giving much lower porosity and permeability. Also the core was extracted in-situ directly without running native state tests. The high recovery by both water flooding and caustic flooding (51% and 31%, respectively) was surprising for this low-permeability core. Extraction of the core after the test confirmed the low residual oil saturation of 18%.

Figure 1 shows the recovery history of core C-1 plotted as fraction of initial oil in place recovered as a function of pore volumes of water and caustic injected. It is interesting to note that no tertiary oil was recovered until nearly 2 1/2 pore volumes of caustic had been injected. It should also be noted that the pH of the effluent remained low until after the first tertiary oil was recovered. This would indicate a very large consumption of caustic (probably most of it being adsorbed by the fine-grained, clayey reservoir rock) before any oil was produced. Thereafter, the pH and recovery curves tend to be parallel. It should be noted that the oil was produced in slugs with no sign of emulsification until the very last oil production increment which was in the form of a small oil slug followed by a very dilute oil in water emulsion.

In Figure 2 the production performance of core A-2 is compared with C-1. Recalling that the A-2 core was much more permeable than C-1, the much earlier recovery (from a pore volume standpoint) might be expected for the A-2 core. The caustic consumption is also much lower in the case of the more permeable core, although the pH and oil recovery curves are again parallel with oil production ceasing as the effluent pH approaches the value for the injected fluid. A possible difference between these two cores is that A-2, the lower caustic consumer, was previously flooded with caustic in the native state and it is possible that all the adsorption had not been reversed.

No sweeping conclusions can be reached from this limited number of tests on oil field cores. However, certain observations seem irrefutable. It is clear that with sufficient initial oil saturation, oil can be recovered in the tertiary mode by caustic injection, at least under laboratory conditions. Consumption of caustic by the fine-grained, clayey reservoir rock is high, especially for the low permeability cores. The recovery mechanism with the oil field cores and fluids does not appear to involve emulsification, at least the vast majority of the oil produced was emulsion-free so that if emulsions were formed in the core, they must have been of the unstable variety. No large changes in pressure gradients were noted which would have occurred if emulsion entrapment were present.

The recovery of tertiary oil appears to be associated with caustic consumption. No oil is recovered until the effective caustic concentration in the core exceeds a critical level. At this point some oil is accumulated and produced in a mini-bank. This process continues in a step-like manner as the critical caustic saturation level is reached progressively down the tube. The recovery mechanism in this case may involve wettability reversal with sharp wettability gradients.

Synthetic System

To understand the complicated chemistry involved in alkali flooding we are studying the displacement of oleic acid-doped mineral oil (1.5 cp and acid #2) from Ottawa sand packs (ca. 5 Darcy) at a scaled rate (7 ft/day). Details of the experimental apparatus and procedures are available (2).

Experimental results for the percentage recovery of oil remaining after water flooding to residual as a function of pH at two NaCl salt contents are shown in Figure 3. Without salt no recovery of tertiary oil is found. As discussed previously (2) nonsaline high pH (ca. 12) solutions lead to core

plugging but not to tertiary oil recovery. However, high saline solutions exhibit recovery which is a strong function of pH. At pH values below about 11 the alkaline solutions are buffered to provide sufficient neutralizing capacity.

Interfacial tensions for the solutions in Figure 3 are all above 0.1 dyne/cm giving Capillary numbers less than 10^{-3}. Hence recovery cannot be explained by the low tension mechanism. Figure 4, however, provides considerable insight into the underlying surface chemistry. For salt solutions below 1 weight percent emulsions are of the oil-in-water type whereas above 1 weight percent they invert to the water-in-oil type. Also above 1 weight percent salt the receding contact angles (measured through the water-phase against quartz) show a reversion to oil-wet. The degree of oil-wetness is a function of solution pH. Note that the degree of oil wettability exactly parallels the recovery efficiencies in Figure 3. In this system only solutions which form water-in-oil emulsions and which exhibit strong oil-wet conditions give tertiary oil production.

It is well documented (4,5) that water-in-oil emulsions in fatty-acid soap systems are stabilized by interfacial films. Although the nature of these films is notwell understood (5), they appear to be caused by a common-ion precipitation at the oil-water interface and may form a surface "precipitate" before bulk precipitation occurs (4):

$$Na^+_{surface} + A^-_{surface} \rightleftarrows NaA_{surface\ film} \qquad (1)$$

Apparently these films also cause oil wettability at the solid-liquid boundary. The dependence of contact angle on pH can be rationalized in terms of the hydroxyl ion controlling the percentages of hydrolyzed (A^-) and unhydrolyzed (HA) fatty-acid at the interface. Considerable evidence exists in flotation studies of the interfacial complex (HA_2^-) at pH's near 8.5 (6).

From these surface chemistry principles we may postulate, but not establish, the governing recovery mechanism. Swelling of the residual oil globules occurs because of water-in-oil emulsification. This swelling in combination with an oil-wet solid matrix permits adjacent globules to contact and form a region of sufficient saturation to permit two-phase flow with establishment of an oil bank. Not all the tertiary oil is recovered because some swollen oil globules are sufficiently far apart that they cannot interconnect, coalescence between contacting globules may be slow, and fingering of the drive alkali may occur. The chemistry embodied in the recovery mechanism suggests that alkali of divalent metal cations, which are known to cause water-in-oil emulsions, should recover tertiary oil. Indeed we have observed that calcium hydroxide will improve oil recovery in the synthetic fatty-acid system.

Displacement Modeling

The displacement of acidic crude oil from a porous medium by an alkaline solution is similar to an immiscible displacement process with chromatographic separation of the surfactant species between the oil, water, and rock phases. If the flow properties in an alkaline flood can be represented empirically by

the relative permeability concept, then it is possible to extend the Buckley-Leverett waterflood theory by allowing the relative permeability to be a function of saturation and concentration of the surfactant generated by the in-situ alkaline chemical reaction. Similar extensions of the Buckley-Leverett equation have been developed for enriched gas drives (7), detergent (8) polymer (9), alcohol (10), carbonated water (11), surfactant (12) and micellar flooding (13).

Figure 5 shows dynamic relative permeability curves (14, 15) for a standard waterflood and a secondary alkaline flood employing 0.1 weight percent NaOH (pH = 12.5) and 5.8 weight percent NaCl with oleic-acid (#2) doped mineral oil (1.5 cp) in an Ottawa sand pack. The solid and dashed lines in this figure correspond to best fits of the empirical forms suggested by Larson and Hirasaki (12):

$$k_{rw} = k^{o}_{rw} \tilde{S}_w^{n}$$

$$k_{ro} = k^{o}_{ro} (1-\tilde{S}_w)^{p} \qquad (2)$$

$$\tilde{S}_w = (S_w - S_{wir})/(1-S_{or}-S_{wir}).$$

Note that the residual oil saturation has not been improved by the alkaline flood in agreement with Figure 3 for a tertiary flood with this same system. If the empirical relative permeabilities for the alkaline flood in Figure 5 are independent of the initial oil saturation (i.e. the displacement mechanism is independent of the amount of oil in the core) then they may be used to represent the behavior of any alkaline flood independent of the water-to-oil ratio at which injection commences. Such an assumption may not be valid when strong emulsification occurs because classical relative permeabilities probably cannot correctly describe emulsion flow behavior (see the section on emulsion flow).

To predict alkaline flooding performance the Buckley-Leverett continuity equations and Darcy's law are solved for a shock condition:

$$\left(\frac{\partial \tilde{x}}{\partial \tau}\right)_{S_{wf}} = \frac{\Delta f_w(\tilde{S}_w, c_{OH^-})}{\Delta \tilde{S}_w} \qquad (3)$$

where Δ indicates a difference across the shock front. We emphasize that the fractional flow curves here are functions of saturation and alkali composition. Thus the transport of the hydroxide ion must be quantified. This is done by writing a species material balance in reduced form:

$$S_w \frac{\partial}{\partial \tilde{\tau}} \left[\tilde{c}_{H^+} - \tilde{c}_{OH^-} + \tilde{c}_{HAw} - \tilde{c}_{HAo}\right] - S_w \frac{\partial \tilde{\Gamma}}{\partial \tilde{\tau}}$$

$$+ f_w \frac{\partial}{\partial \tilde{x}} \left[\tilde{c}_{H^+} - \tilde{c}_{OH^-} + \tilde{c}_{HAw} - \tilde{c}_{HAo}\right] + \frac{\partial \tilde{c}_{HAo}}{\partial \tilde{x}} = 0 \qquad (4)$$

Next, instantaneous equilibrium with no adsorption of HA and A^- is assumed:

$$\begin{aligned} HA_w &\overset{K_D}{\rightleftarrows} HAo \quad , \\ HA_w &\overset{K_A}{\rightleftarrows} H^+ + A^- \quad , \\ H_2O &\overset{K_w}{\rightleftarrows} H^+ + OH^- \quad , \\ \tilde{\Gamma} &= \frac{a_L \, c_{OH^-}}{1 + b_L \, \tilde{c}_{OH^-}} \quad , \end{aligned} \qquad (5)$$

and electroneutrality in the bulk solution and at the aqueous solid-liquid boundary is imposed. For excess added salt equations (4) and (5) combine to give also a shock-front solution:

$$\left(\frac{\partial \tilde{x}}{\partial \tilde{\tau}}\right)_{\tilde{c}_{OH}} = \frac{\Delta f_w + \Delta \tilde{c}_{HAo} / \Delta\left[\tilde{c}_{H^+} - \tilde{c}_{OH^-} + \tilde{c}_{HAw} - \tilde{c}_{HAo}\right]}{\Delta S_w + \Delta\left[\tilde{c}_{HAo} - S_w \tilde{\Gamma}\right] / \left[\tilde{c}_{H^+} - \tilde{c}_{OH^-} + \tilde{c}_{HAw} - \tilde{c}_{HAo}\right]} \qquad (6)$$

Equations (3), (5), and (6) in conjunction with Figure 5 suffice to predict the saturation and pH profiles in an alkaline flood.

Figure 6 gives predicted saturation and pH profiles for a caustic flood with relative permeability curves corresponding to Figure 5. All the parameters embodied in equation 5 are obtained by independent experiments. The alkaline flood encounters a core with a 50 percent oil saturation and the two cases of caustic adsorption and no caustic adsorption are compared. Note that adsorption causes the pH and saturation profiles to lag and delay production. Also an oil bank is formed directly in front of the caustic. Figure 7 gives similar profiles for the relative permeability curves of Figure 5 with a hypothetical residual oil saturation of 0.1. Finally Figure 8 summarizes the production history of Figures6 and 7. Although, in this case, the caustic flood with $S_{or} = 0.27$ does not displacc any more oil than a plain waterflood, the production occurs earlier as in a polymer flood. This production advantage is somewhat offset when caustic adsorption is included. Since caustic adsorption on Ottawa sand is minimal, larger production delays can be expected in actual reservoir sands.

The present treatment is preliminary in that a number of simplifications are invoked in the instantaneous equilibria of equation 5. The most questionable assumption is the validity of relative permeabilities in alkaline flooding, especially if strong emulsification occurs. However, this displacement model serves a basis for handling more realistic assumptions.

INTERFACIAL TENSION

Crude Oil

Spinning drop (16) interfacial tensions of Ranger-zone crude oil against different sodium hydroxide solutions are shown in Figure 9 at ambient temperature. As previously observed (2, 17) acid crude-oil tensions show a dynamic minimum. For the ultralow tensions the return to high tension is not experimentally available. This is because the contracting drop succumbs to inevitable external disturbances and breaks into satellite drops.

Figure 9 also indicates the sensitivity of the minimum dynamic tension to small changes in hydroxyl ion concentration. This sensitivity to pH is further accentuated in Figure 10 which gives the minimum tension as a function of caustic pH. Here the narrow range of ultralow tensions typical of synthetic surfactants is evident.

The effect of aqueous salt content and pH on Ranger-zone crude oil minimum dynamic tension is portrayed in Figure 11. Addition of sodium chloride shifts the pH for dynamic minimum tensions less than (10^{-3}) dyne/cm to lower values. Also for the lower salt concentrations the 10^{-3} dyne/cm isotension well broadens. Similar general conclusions can be drawn from the data of Jennings (18). One important result from Figure 11 is that the original THUMS flood design does not appear to fall in the lower tension composition region (i.e. pH $\sim$ 12.5 and [NaCl] = 1 wt%).

Dynamic Tensions

Previous reports (2) as well as literature work (17, 19, 20, 21) show that "dynamic" tensions can exhibit a sharp minimum. This minimum is especially dramatic when an acidic California crude oil or synthetic oils containing an oil-soluble hydrolyzable surfactant are brought in contact with an aqueous alkaline solution (see Figure 9). An appropriate explanation of this tension minimum is important not only in the proper interpretation of interfacial tension measurements, but also in the potential exploitation of this phenomena for enhanced oil recovery.

A minimum in dynamic tension is indicative of a period where surfactant concentration at the interface reaches a maximum value (2). During this time period, emulsification into small oil droplets can occur with negligible shear energy input (e.g. spontaneous emulsification). If the duration of low interfacial tensions is long enough, emulsification may be possible with very low acid concentrations in the oil phase. However, if after the minimum the tension rapidly rises back to a high value, propagation of the entrained droplets cannot take place except through the larger pores or by coalescence

into an oil bank. A low tension minimum followed by a rapid rise to a high equilibrium tension seems well-suited to the entrapment recovery mechanism.

To understand the origin of dynamic tension minima, or equilvalently, surface adsorption maxima, a theoretical analysis has been developed. Following the work of England and Berg (21) a five step kinetic sequence with sorption barriers was previously outlined (2). In addition a major factor in the appearance, duration and value of the tension minimum in the present work is the volume of the two phases, as well as sorption barriers and interfacial area. This is true in the spinning-drop tensiometer, as well as in oil reser voirs where a certain average finite volume of aqueous phase can conceptually be assigned to each entrapped oil ganglia. The details of the model and the mathematical derivation are now in the final stages of preparation for publication.

The main assumptions in the model are the following. The two phases have finite volume V_1 and V_2 (phase 1 is the oil phase and phase 2 is the water phase) with an interfacial area A. Each well-mixed phase contains an average surfactant concentration c_1 and c_2 with phase 1 containing initially all the surfactant solute. Solute is transferred into phase 2 through the interface where adsorption-desorption kinetics of the first order prevail:

$$\text{surfactant in oil} \underset{k_{-1}}{\overset{k_1}{\rightleftarrows}} \text{surfactant adsorbed} \underset{k_{-2}}{\overset{k_2}{\rightleftarrows}} \text{surfactant in water} \qquad (7)$$

Unsteady state material balances are written for each of the phases and for the interface. The resulting system of simultaneous differential equations for a constant area drop admits an analytic solution to predict reduced adsorption, Γ^*, as a function of reduced time, t^*:

$$\Gamma^* = Ae^{at^*} + Be^{bt^*} + \Gamma^*_\infty \qquad (8)$$

where Γ^*_∞ is the equilibrium value of Γ^* and A, B, a and b are constants related to three dimensionless parameters. One parameter characterizes the kinetics: $\kappa = k_{-1}/(k_{-1}+k_2)$; and two parameters characterize the equilibrium state: $\alpha = K_D A/V_1$; $\beta = HA/K_D V_2$, where H is Henry's adsorption constant and K_D is Nernst's distribution coefficient. Finally, the surface excess adsorption in equation (8) can be related to the dynamic interfacial tension using the assumption of instantaneous surface equilibrium and the Gibbs adsorption isotherm:

$$\frac{\gamma}{\gamma_o} = 1 - \delta\Gamma^* \qquad (9)$$

where γ_o is the initial interfacial tension between the pure phases (no solute) and δ is an additional dimensionless parameter relating the initial interfacial tension to the initial amount of surfactant in the oil phase. Equations (8) and (9) provide a means for theoretical prediction of the time evolution of the interfacial tension.

Figure 12 shows typical results for the time behavior of the reduced surface excess adsorption for given α and β with various reduced sorption barrier constants κ. Note that a large transient maximum in Γ^* appears when a large desorption barrier exists on the water side of the interface (i.e. κ approaches unity). Figure 12 also indicates that the larger the maximum value of Γ^* the longer is the relative duration of these high values. Of course, as the desorption barrier diminishes (i.e. κ approaches zero) no maxima are evident.

Figure 13 depicts the importance of the volume of water surrounding an oil droplet. Small values of β correspond to larger water volumes such as in the spinning drop tensiometer where the volume of water to oil ratio is above 100. Here once a minimum tension is reached the tension returns almost to its original value. This is because the copious amount of water dilutes the fixed amount of surfactant in the system. As the volume of water lessens (i.e. β increases) the final equilibrium tension plummets to about the minimum value obtained for high water volumes. Thus, the time evolution tension curve from a spinning-drop tensiometer is not characteristic of that in an oil reservoir where the volume of water to oil ratio is about 3. However, the spinning-drop tension minimum does appear to be characteristic. Thus, the present simplified model untangles some of the puzzling results obtained in interfacial tension measurements and it indicates direction for application of these results.

EMULSION FLOW AND STABILITY

Porous Media Flow

Two of the fundamental oil recovery mechanisms that have been suggested for alkali flooding involve emulsions (1). These are emulsification and entrainment and emulsification and entrapment. The former was first discussed by Subkow (22), who believed that the crude oil is emulsified in-situ by lowering the interfacial tension and then entrained as a continuous flowing alkaline water phase. This mechanism precludes any increase in recovery before caustic breakthrough, and the oil recovery is as an emulsion flowing with the caustic front. The latter mechanism was proposed by McAuliffe (23, 24), who noted that the size of the emulsion droplets generated in-situ is not small enough to penetrate through all small pore-throat constrictions. Instead entrapment occurs between sand grains. This causes a reduction of water mobility and leads to an increase in sweep efficiency and oil recovery in the low permeability zones of the reservoir. The entrapment mechanism results in no significant reduction in ultimate residual oil saturation, but rather it reduces the water-oil ratio required to reach this residual oil saturation. The oil recovered from this mechanism is as a separate phase.

The primary differences between these two mechanisms are the interfacial tension and the ratio of drop sizes to pore sizes. High interfacial tension and large drop-size to pore-size ratio will result in the entrapment mechanism and low interfacial tension and small drop-size to pore-size ratio will exhibit

the entrainment mechanism. Thus, the purpose of this work is to study the effect of interfacial tension and drop-size to pore-size ratio on emulsion flow through porous media.

An experimental system has been constructed, as described previously (2), to obtain the pressure drop-flow rate relations for dilute stable emulsion flow in consolidated and unconsolidated porous media. Further a quantitative model, based on deep bed filtration theory, has been developed to describe the bed permeability. The rudiments of this theory have been enunciated (2) and the details will be available in a forthcoming manuscript. The model leads to a nonlinear partial intergro-differential equation which may be solved by a modified method of characteristics (25) to yield:

$$\frac{K_o}{K(\tau)} = 1 - \tilde{x} + \int_{\sigma_o}^{\sigma_x} \frac{\phi_o \, d\sigma}{\sigma(\phi_c - \sigma)\Lambda} , \tag{10}$$

where

$$\tilde{x} = \int_{\sigma_x}^{\sigma_i} \frac{(\phi_o - \sigma) \, d\sigma}{(\phi_c - \sigma)\sigma\Lambda} , \tag{11}$$

and

$$\tau = \int_{o}^{\sigma_i} \frac{(\phi_o - \sigma_i) \, d\sigma_i}{\phi_o \, \Lambda \, f_i(\phi_c - \sigma)} . \tag{12}$$

In these equations ϕ_c is a critical porosity and is a complicated function of the Capillary number and the pore-size distribution. Equations (10) to (12) may be evaluated numerically to predict the porous medium permeability as a function of injected pore volumes of emulsion, τ.

Figures 14 and 15 show typical results for a Gaussian pore-size distribution with a dimensionless variance of 0.5. The extreme sensitivity of the core permeability to the average drop-size to pore-size ratio is shown in Figure 14. This figure also shows that the difference between entrainment and entrapment flow is one of degree with large drops in low permeability media showing relatively more entrapment than small drops in high permeability media. Conversely, Figure 15 shows the relative insensitivity of core permeability to droplet interfacial tension (through the Capillary number). Only for extremely low interfacial tensions (i.e. very high Capillary numbers) can entrainment flow be expected when droplets must squeeze through pore constrictions.

Emulsion Stability

Emulsion stability plays an important role in determining oil recovery mechanisms (1). Unstable emulsions allow oil drops to coalescence and form an oil continuous bank. Conversely, stable emulsions may increase recovery by the entrainment and/or entrapment mechanisms. Therefore, an accurate and reliable method is needed to characterize quantitatively emulsion stability.

Currently, three techniques exist to measure emulsion stability. These are: (1) coalescence time of an oil drop at a flat oil-aqueous interface (26, 27, 28), (2) microscopic counting of drops as a function of time (29) and (3) collection of a coalesced oil phase in a centrifugal field (30). The first method suffers from its statistical nature and lack of reproducibility. Both the first and second methods require a long experimental times (up to weeks) due to the emulsions generated from alkaline flooding being quite stable. The centrifuge method, which has the advantage of convenience and speed, has, however, the difficulty of data interpretation owing to the ambiquity of the controlling coalescence mechanism. The purpose of this work is to investigate the dominant mechanism which controls the rate of oil separation.

Mineral oil in water emulsions, stabilized by sodium oleate, were tested in an ordinary laboratory centrifuge. Results for the volume of coalesced oil as a function time are shown in Figures16 and 17 for two average drop sizes (determined by photomicroscopy) and for several centrifugal field strengths. Note that the volume of oil collected is a linear function of time indicating that coalescence is occurring mainly at the oil-water interface and not in the creamed layer. An increase either in drop size or centrifugal field causes an increase in coalescence rate.

Two simplified models have been developed to describe the results of Figures 16 and 17. The first one takes film thinning as the rate-determining step for coalescence and utilizes the classic expression for the coalescence time of an undeformable spherical drop at a flat interface (26). Thus the rate of oil collection is

$$\frac{dV}{dt} = \frac{8\ R^2\ A\ \Delta\rho\ Ng\ (1-\eta)}{27\ \mu \ln\ (h_o/h_c)} \tag{13}$$

Alternately, if drainage through a packed bed of undeformable spheres is the coalescence controlling step, then the rate of oil collection may be given by

$$\frac{dV}{dt} = \frac{R^3\ A\ \Delta\rho\ Ng\ (1-\eta)}{45\ \mu(h_o-h_c)} \tag{14}$$

Both models show a linear dependence on centrifugal force and a strong drop size dependence. Unfortunately, data obtained to date cannot distinguish unambiguously between or reject either of the two models. Thus, although accurate emulsion stability from the centrifuge method is readily obtained, further work is needed to establish a correlation with emulsion stability in an oil reservoir.

CAUSTIC LOSS

In this work caustic consumption by reservoir rock is measured by frontal-analysis chromatography using a liquid chromatograph. This allows determination of both equilibrium consumption and band-broadening resistances in the same experiment. Equilibrium loss is obtained from the solute-residence time of an input concentration step-change and an overall solute material balance (31).

$$\frac{ma_s}{\phi AL}\frac{\Delta\Gamma}{\Delta c} = \tau_R - 1 \quad , \tag{15}$$

where τ_R the solute residence time (or pore volumes to breakthrough) is calculated from the elution curve according to

$$\tau_R = \frac{Q}{\phi A\, L}\left[\frac{c_i t_\infty - \int_o^{t_\infty} c_{out}(t)\,dt}{c_i - c_o}\right] \tag{16}$$

Notice first that $\Delta\Gamma/\Delta c$ represents a cord of the adsorption isotherm. Thus, the number of pore volumes before breakthrough is not a direct indication of the amount adsorbed. In fact, typical adsorption isotherms have monotonically decreasing slopes and therefore require fewer pore volumes for breakthrough as the amount adsorbed increases. Second, equation (16) reveals that concentrations and notpH values (15) should be used in determining the pore volumes for response, τ_R. Use of pH instead of concentration always under-estimates alkali loss and we find that errors of up to 50% can readily occur. Strictly, pH measures hydrogen ion activity not concentration so that an activity coefficient correction is required. However, in nonsaline solutions of moderate pH this correction is not large.

Adsorption of sodium hydroxide on oil-free Ranger-zone sand at 20°C is shown in Figure 18. Because hydroxyl and hydrogen ion concentrations are never independent, the adsorption in Figure (16), Γ, is actually the difference between hydroxyl ion adsorption ($\Gamma \equiv \Gamma_{OH^-} - \Gamma_{H^+}$) and not the hydroxyl ion adsorption alone. Further, Γ is measured relative to water of pH seven as hydroxyl ion concentration in water is always finite. Experimental data in Figure 18 include those obtained after reflushing the column to neutral pH thus indicating reversible caustic adsorption at ambient temperature. The alkali adsorption loss given in Figure 18 falls in line with other reported reservoir data (32). However, Figure 18 shows the strong influence of hydroxyl concentration.

The elution curve also gives information on adsorption kinetics. For simple external mass transfer controlled adsorption in the linear Henry law isotherm region, Thomas' analytical solution is applicable (33). Figure 19 compares the experimental caustic elution curve to the theoretical calculation with the mass transfer coefficient estimated from the work of Tiedemann and Newman (34). Clearly external mass transfer (and/or axial dispersion) cannot explain the observed spread and additional resistances must be considered. The most likely, but unexpected, candidate is an internal particle mass transfer resistance suggesting porous solids in the Ranger-zone sand. This possibility

is strengthened by the high specific surface area of this sand (ca. 7 $m^2 gram^{-1}$ by nitrogen BET) with particle sizes between 10 and 100 μm.

Considerable evidence indicates that caustic loss increases dramatically as a function of temperature (35). This work is pursuing both the kinetic and equilibrium aspects of the temperature dependence of alkali loss using frontal-analysis chromatograph.

TABLE 1. Ranger-zone Core Floods

Test	Condition	ϕ	K mD	S_{wi}	S_{oi}	E_{rw}	E_{rc}
A1	Native	.35	-	.24	.25	0	0
A2	Resat.	.36	460	.26	.74	.46	.66
B1	Native	.39	-	.40	.24	0	0
B2	Resat.	.40	430	.43	.57	.27	.37
C1	Resat.	.27	65	.43	.57	.51	.82

NOMENCLATURE

a, A	constants in Equation 8.
a_L	Langmuir adsorption constant
a_s	solid surface area, m^2/g
A	cross-sectional area, m^2
b, B	constants in Equation 8
b_L	Langmuir adsorption constant
c	concentration, moles/liter
$\tilde{c}$	reduced concentration, $c/\sqrt{K_w}$
Ca	dimensionaless Capillary number, $\mu u/\phi_o \gamma$
Dd	drop diameter, m
$<D_p>$	average pore diameter, m
E_{rw}	waterflood recovery efficiency
E_{rc}	chemical recovery efficiency
f_i	inlet emulsion volume fraction
f_w	fractional flow of water
h	film thickness, m
H	Henry adsorption constant, m
$k_1, k_2, k\text{-}1, k\text{-}2$	reaction rate constants, sec^{-1}
k_r	relative permeability
K	permeability, m^2
K_A	acid dissociation constant, moles/liter
K_D	distribution coefficient
K_w	water dissociation constant, $moles^2/liter^2$
L	core length, m
m	mass of solid kg
M	molarity
Ng	centrifugal force (number of gravities), kgm/sec^2
n,p	constants in Equation (2)
O/W	oil in water
Q	volumetric flow rate, m^3/sec
R	drop radius, m
S	saturation, volume of fluid/void volume
t	time, sec
t^*	reduced time, $t(k_{-1}+k_2)$
u	superficial velocity, m/sec

W/O	water in oil
$\tilde{x}$	reduced axial coordinate, x/L

Greek Symbols

α	reduced oil volume, $K_D A/V_1$
β	reduced water volume $HA/K_D V_2$
γ	oil-water interfacial tension
Γ	caustic adsorption (Γ_{OH} - Γ_{H+}), moles/m^2
$\tilde{\Gamma}$	reduced caustic adsorption, $\frac{(1-\phi)\ \rho_s \Gamma}{\phi\ Sw\ \sqrt{Kw}}$
Γ^*	reduced surfactant adsorption at the oil-water interface
δ	reduced initial interfacial tension, equation 9
η	two-dimensional void fraction
κ	reduced rate constant, k-1/(k-1 +k_2)
Λ	reduced filter coefficient
μ	viscosity, cp
ρ	density, kg/m^3
σ	local oil retention, oil volume/bed volume
τ	pore volumes injected or dimensionaless time, $ut/\phi_o L$
τ_R	reduced residence time
ϕ	bed porosity, void volume/bed volume

Subscripts		Superscripts	
1	oil phase	o	end point
2	water phase	~	reduced
c	critical	*	reduced
f	front		
i	inlet or initial		
ir	irreducible		
min	minimum		
o	oil or initial		
or	residual oil		
out	outlet		
s	solid		
w	water		
x	axial position		
∞	infinity		

ACKNOWLEDGEMENT

The authors are grateful for the financial support of the Department of Energy (Contract No. W-7405-ENG-48). Also the close liaison with Mr. Dave Rowland of the San Francisco Office of DOE is appreciated.

REFERENCES

1. Johnson, C. E., Jr.: "Status of Caustic and Emulsion Methods," J. Pet. Tech., (Jan. 1976) 85-92.

2. Radke, C. J. and Somerton, W. H.: "Enhanced Recovery with Mobility and Reactive Tension Agents," Third ERDA Symposium on Enhanced Oil and Gas Recovery and Improved Drilling Methods", Tulsa, Vol. 1, p. B-5 (1977).

3. The City of Long Beach, Dept. of Oil Properties, Technical Proposal: "Improved Secondary Oil Recovery by Controlled Water Flooding Pilot Demonstration," prepared for the Energy Research and Development Administration under contract no. E(49-18)-2296.

4. Schulman, J. H. and Cockbain, E. G.: "Molecular Interactions at Oil/Water Interfaces, Part II. Phase Inversion and Stability of Water in Oil Emulsions," Trans. For. Soc., 36, (1940) 661-668.

5. Albers, W. and Overbeek, J. Th. G.: "Stability of Emulsions of Water in Oil, I. The Correlation Between Electrokinetic Potential and Stability," J. Colloid and Interface Sci., 14 (1959) 501-509.

6. Somasundaran, P., Ananthapadmanabhan, K. P. and Kulkarni, R. D.: "Flotation Mechanism Based on Ionomolecular Complexes," presented at the Twelfth International Mineral Processing Congress, San Paulo, Brazil (1977).

7. Welge, H. J., Johnson, E. F., Ewing, S. P. Jr., Brinkman, F. H.: "The Linear Displacement of Oil from Porous Media by Enriched Gas," JPT (August, 1961) 787-796.

8. Fayers, F. J. and Perrine, R. L.: "Mathematical Description of Detergent Flooding in Oil Reservoirs," Trans. AIME, 216, (1959) 277-283.

9. Patton, J. T., Coats, K. H., and Colegrove, G. T.: "Prediction of Polymer Flood Performance," Soc. Pet. Eng. J. (March, 1971) 72-84.

10. Wachmann, C.: "A Mathematical Theory for the Displacement of Oil and Water by Alcohol," Soc. Pet. Eng. J. (September, 1964) 250-266.

11. Claridge, E. L. and Bondor, P. L.: "A Graphical Method for Calculating Linear Displacement with Mass Transfer and Continuously Changing Mobilities," Soc. Pet. Eng. J. (December, 1974) 609-618.

12. Larson, R. G. and Hirasaki, G.: "Analysis of the Physical Mechanisms in Surfactant Flooding," SPE 6003, prepared for the 51st Annual Fall Technical Conference and Exhibition of the Society of Petroleum Engineers of AIME, New Orleans, (Oct. 3-6, 1976).

13. Kremesec, V. J. and Treiber, L. J.: "Effect of System Wettability on Oil Displacement by Micellar Flooding," Soc. Pet. Eng. Paper #6001, prepared for the 51st Annual Fall Technical Conference and Exhibitor of the Society of Petroleum Engineers of AIME, New Orleans, (Oct. 3-6, 1976).

14. Johnson, E. F., Bossler, D. P. and Naumann, V. O.: "Calculation of Relative Permeability for Displacement Experiments," Trans. AIME, 216 (1959) 370-372.

15. Jones, S. C. and Roszelle, W. O.: "Graphical Techniques for Determining Relative Permeability from Displacement Experiments," J. Pet. Tech. (May 1978) 807-817.

16. Cayias, J. L., Schechter, R. S. and Wade, W. H.: "The Measurement of Low Interfacial Tension via the Spinning Drop Technique," from Adsorption at Interfaces, A.C.S. Symposium Series 8 (1975).

17. McCaffery, F. G.: "Interfacial Tensions and Aging Behavior of Some Crude Oils Against Caustic Solutions." J. Can. Pet. Tech. (July-Sept 1976) 1-4.

18. Jennings, H. Y., Jr.: "A Study of Caustic Solution-Crude Oil Interfacial Tensions," Soc. Pet. Eng. J. (June 1975) 197.

19. Farmanion, P.A., Davis, N., Kwan, K.T., Yen, T.F., and Weinbrandt, R.M.: "Isolation of Native Petroleum Fractions for Lowering Interfacial Tensions in Aqueous-Alkaline Systems," presented at the Chemistry of Oil Recovery Symposium, American Chemical Society, Anaheim, Ca., (March 1978).

20. Mansfield, W.W.: "The Spontaneous Emulsification of Mixtures of Oleic Acid and Paraffin Oil in Alkaline Solutions," Australian Journal of Sci. Res. Sec. A, Physical Sciences, 5, (1952) 331-338.

21. England, D.C. and Berg, J.C.: "Transfer of Surface Active Agents Across a Liquid-Liquid Interface," AIChE Journal, 17(2), (March 1971) 313.

22. Subkow, P.: "Process for the Removal of Bitumen from Bituminous Deposits." U.S. Patent No. 2288857 (July, 7, 1942).

23. McAuliffe, C.D.: "Oil-in-Water Emulsion and Their Flow Properties in Porous Media," J. Pet. Tech. (June, 1973) 727-733.

24. McAuliffe, C.D.: "Crude-Oil-in-Water Emulsion to Improve Fluid Flow in an Oil Reservoir," J. Pet. Tech (June, 1973) 721-726.

25. Herzig, J.P., Leclerc, D.M. and Le Goff, P.: "Flow of Suspensions Through Porous Media-Application to Deep Filtration," I&EC, 62(5), (1970) 8-35.

26. Charles, G.E. and Mason, S.G.: "The Coalescence of Liquid Drops with Flat Liquid/Liquid Interfaces," J. Coll. Sci. 15, (1960) 236-267.

27. Lee, J.C. and Woods, D.R.: "The Effect of Surfactants on the Coalescence of a Drop at an Interface," J. Colloid and Interfacial Sci. 30 (1969) 429.

28. Vrij, A. and Overbeek, J.Th.G.: "Rupture of Thin Liquid Films Due to Spontaneous Fluctuations in Thickness," J. Am. Chem. Soc., 90, (1968) 3074.

29. Wasan, T.D., Shah, S.M., Chan, M., Sanpath, K., and Shah, R.: "Observations on Emulsion Stability and Interfacial Properties in Improved Oil Recovery by Chemical Flooding," presented at the Symp. on Chemistry of Oil Recovery, Anaheim, March 12-17, 1978. ACS Symposium Series Preprints Volume 23(No. 12)(March, 1976).

30. Mittal, K.L., "Ultracentrifugal Technique in Study of Emulsions," from A.C.S. Symposium Series 9 (1975) 76-95.

31. Wang, H.L., Duda, J.L. and Radke, C.J.: "Solution Adsorption from Liquid Chromatography," J. Colloid Int. Sci., in press (1978).

32. Jennings Jr., H.Y., Johnson Jr., C.E., and McAuliffe, C.D.: "A Caustic Waterflooding Process for Heavy Oils," J. Pet Tech. 126(12) (1974) 1344-1352.

33. Sherwood, T.K., Pigford, R.L., and Wilke, C.R., Mass Transfer, McGraw-Hill (1975) 581, 15-17.

34. Newman, John and Tiedemann, William: "Flow-Through Process Electrodes," Advances in Electrochemistry and Electrochemical Engineering, Vol. 11 (1978) 353-438.

35. Robinson, R.J., Bursell, C.G., and Restine, J.L.: "A Caustic Steamflood Pilot-Kern River Field," SPE 6523 preprint prepared for the 47th Annual California Regional Meeting of the SPE of AIME, Bakersfield, California (April 13-15, 1977).

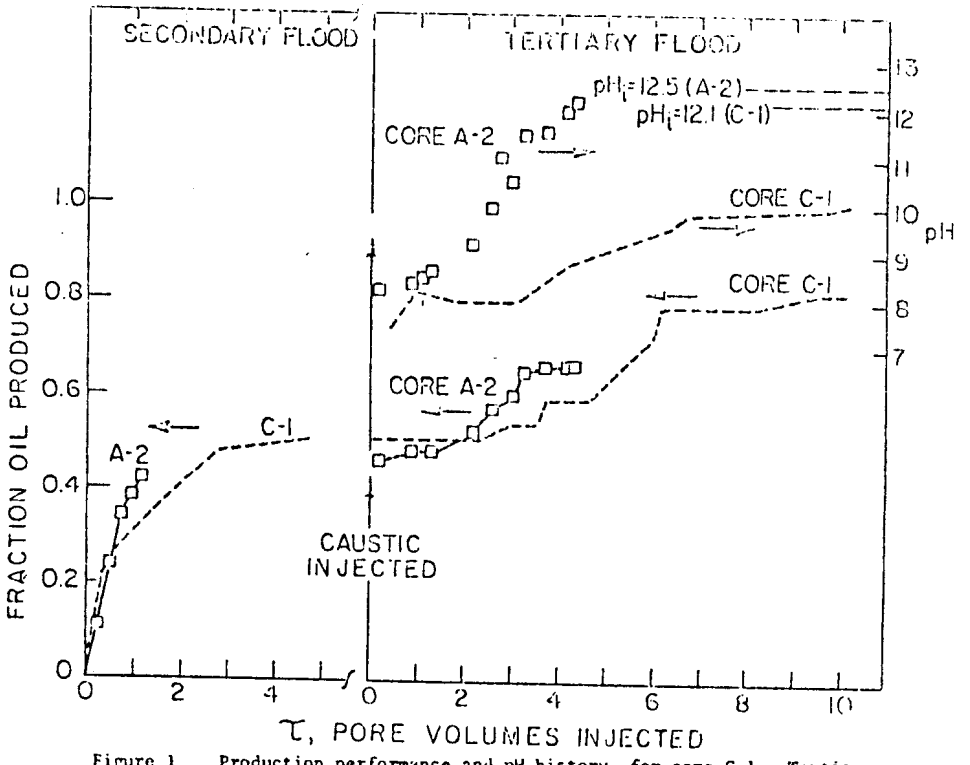

Figure 1 Production performance and pH history, for core C-1. Tertiary flood is 0.2 PV of 1 wt% NaOH followed by 0.1 wt% NaCl with 1 wt% NaOH.

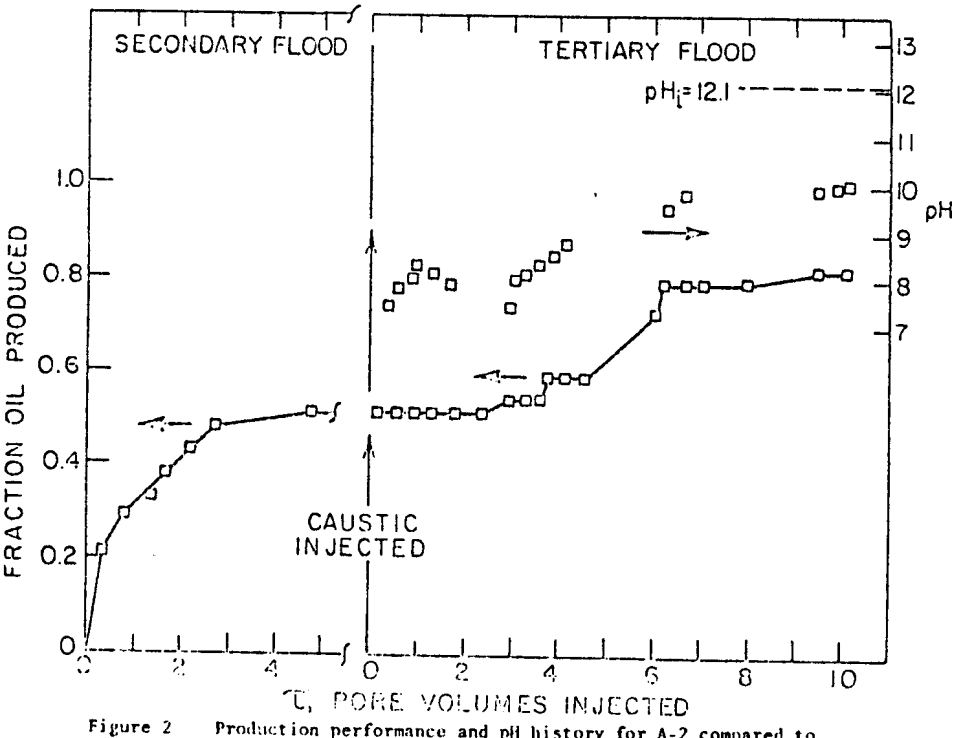

Figure 2 Production performance and pH history for A-2 compared to core C-1

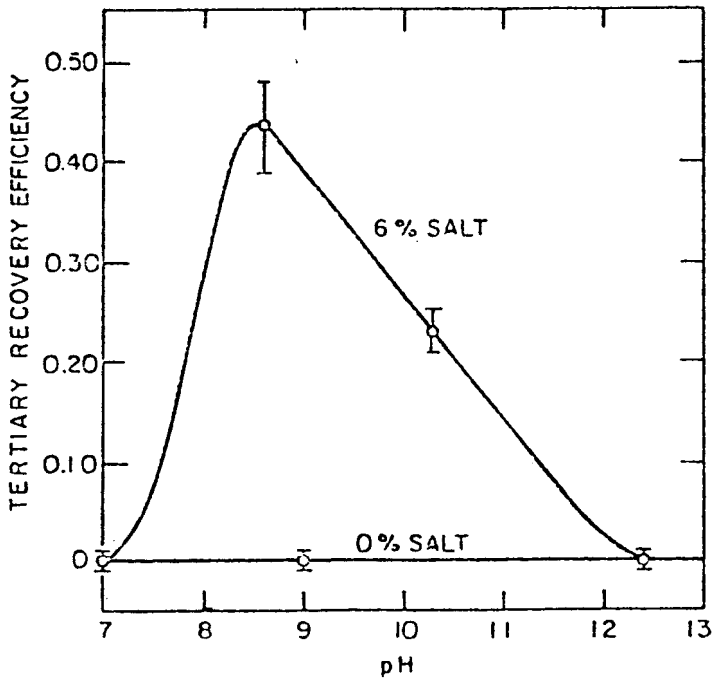

Figure 3 Tertiary recovery efficiency as a function of pH for two salt weight concentrations.

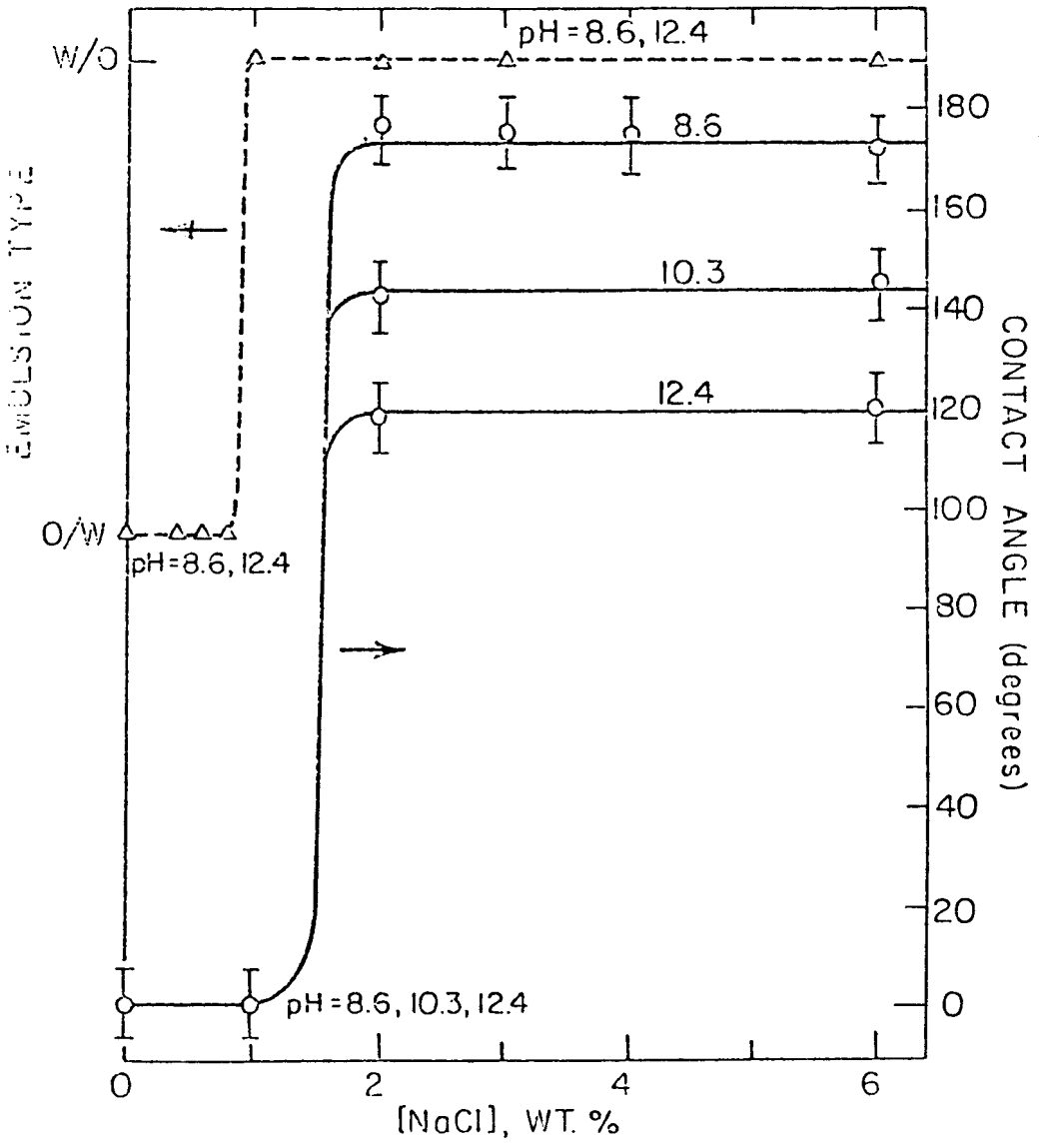

Figure 4. The effect of salt on emulsion type and contact angle.

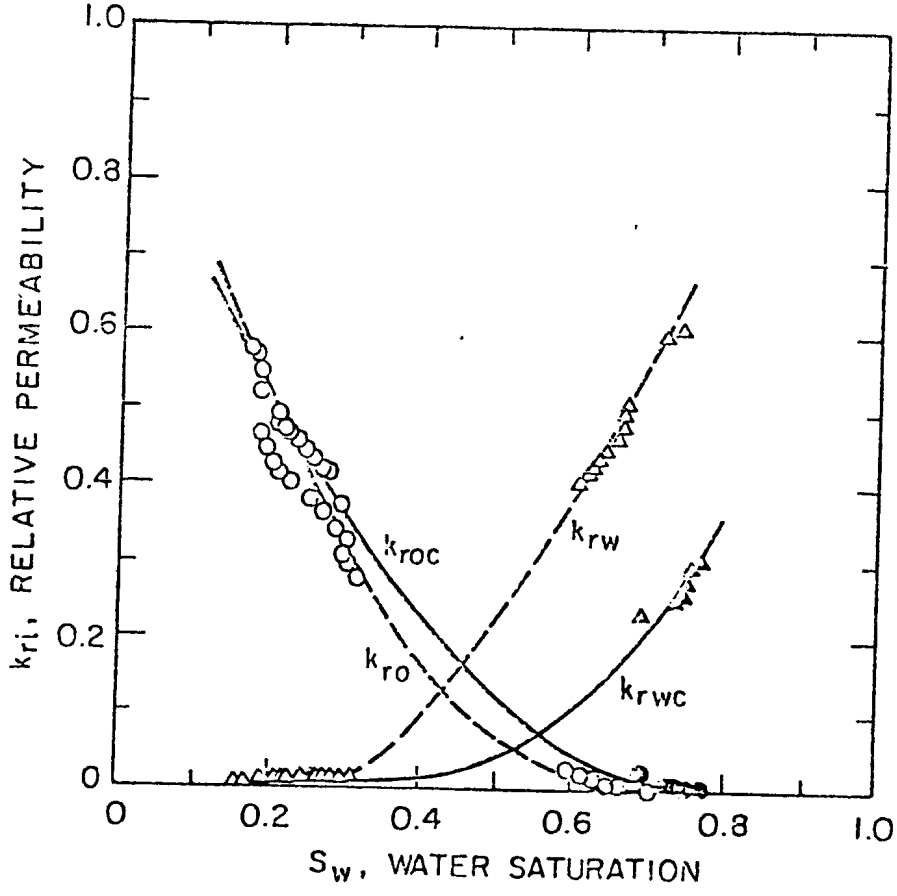

Figure 5. Relative permeabilities for a waterflood and a secondary caustic flood (0.1% NaOH, 5.8 wt% NaCl).

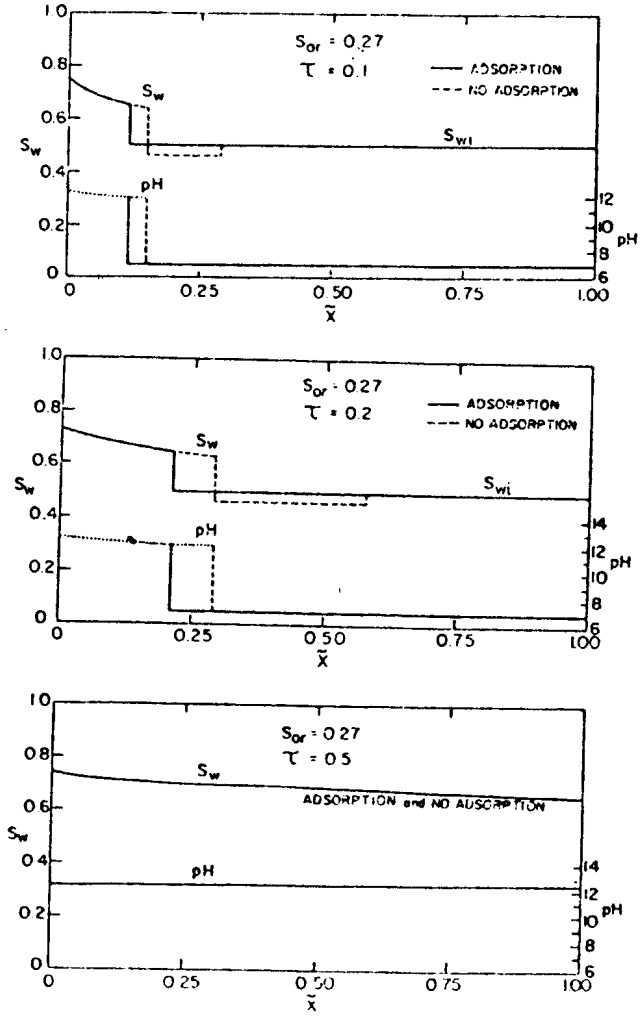

Figure 6. Calculated saturation and pH profiles with and without caustic adsorption (S_{or} = 0.27).

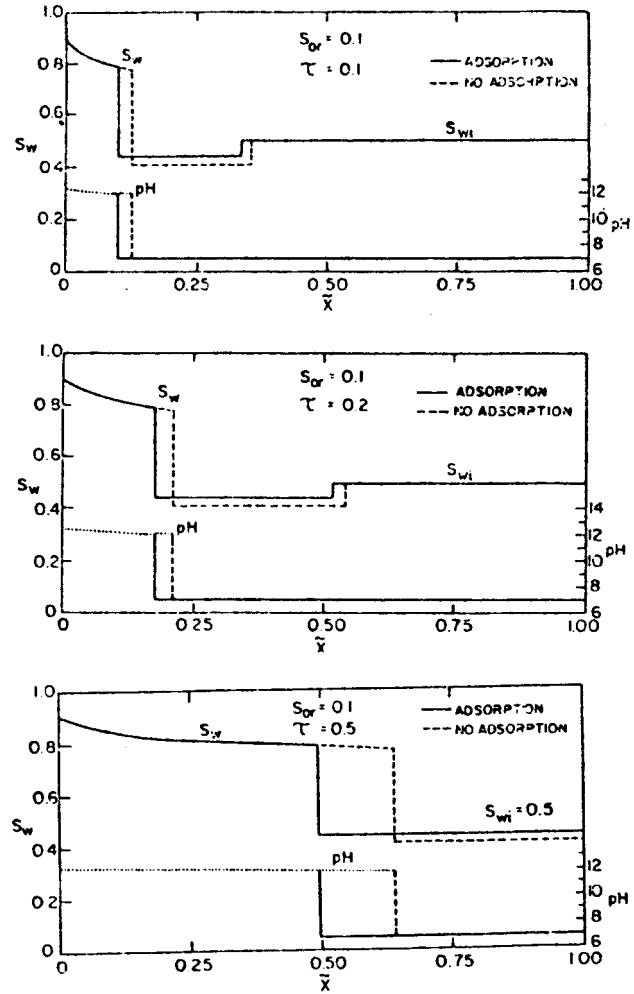

Figure 7 Calculated saturation and pH particles with and without caustic adsorption (S_{or} = 0.1).

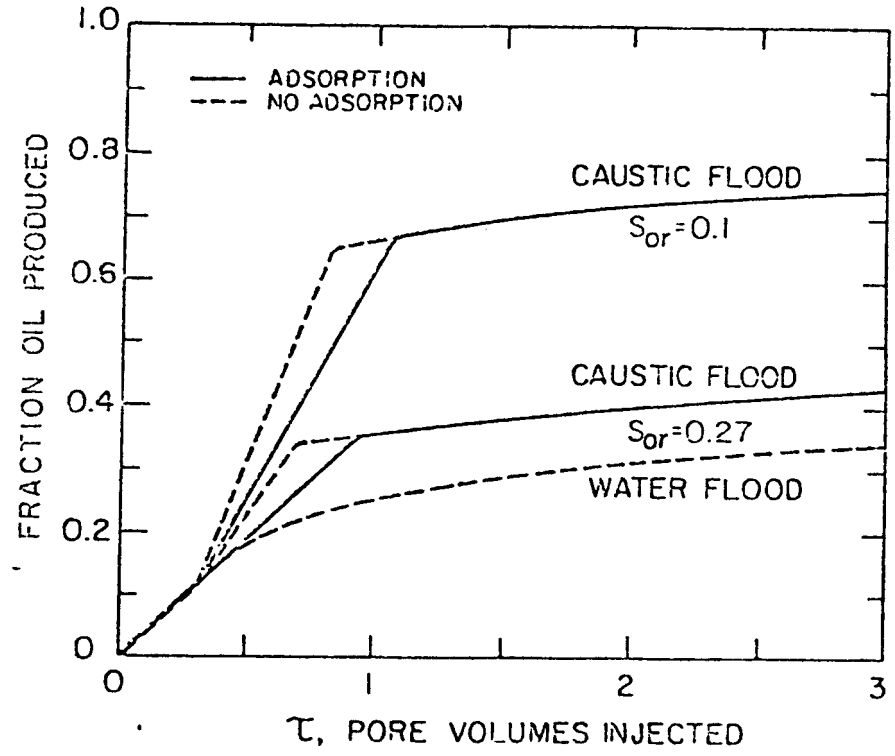

Figure 8 Calculated fractional recovery of oil for a waterflood and two caustic floods (S_{or} = 0.27 and 0.1).

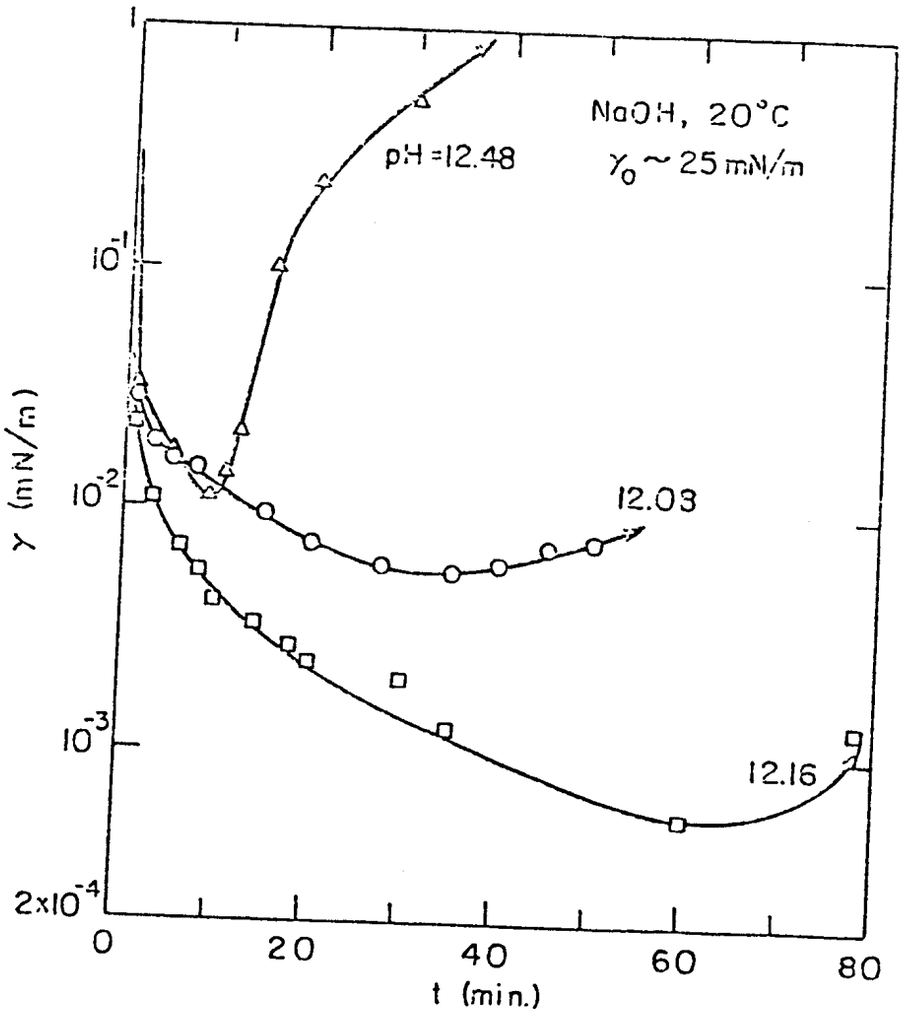

Figure 9 Dynamic tensions as functions of pH for Ranger-zone crude oil.

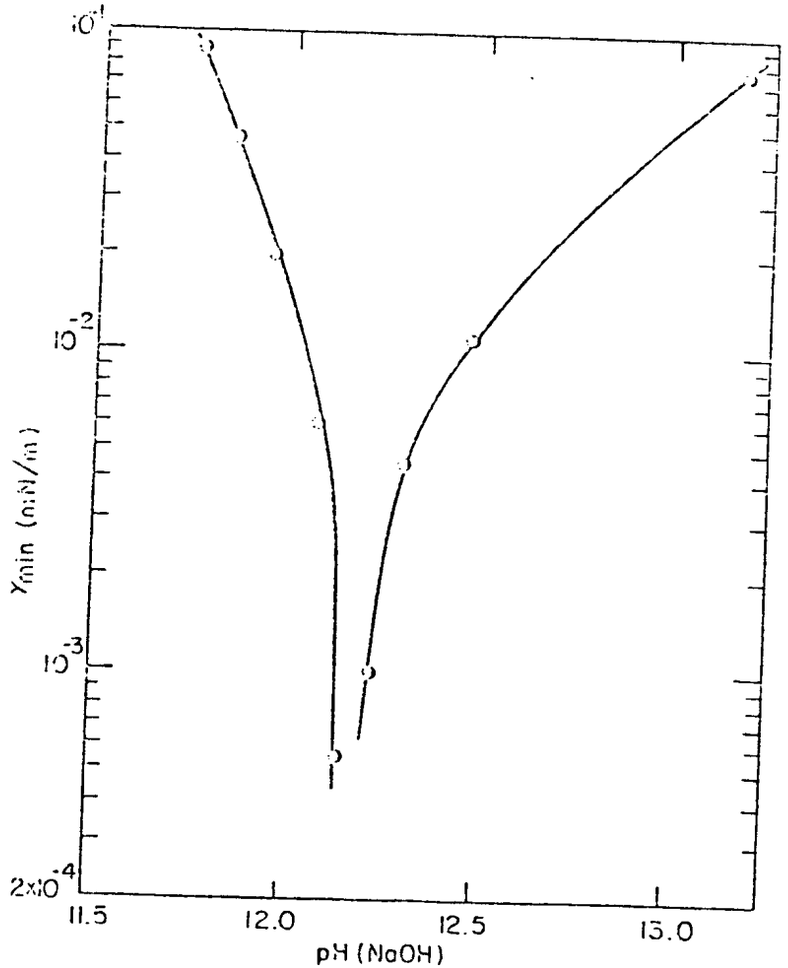

Figure 10 Minimum in dynamic tensions as a function of pH.

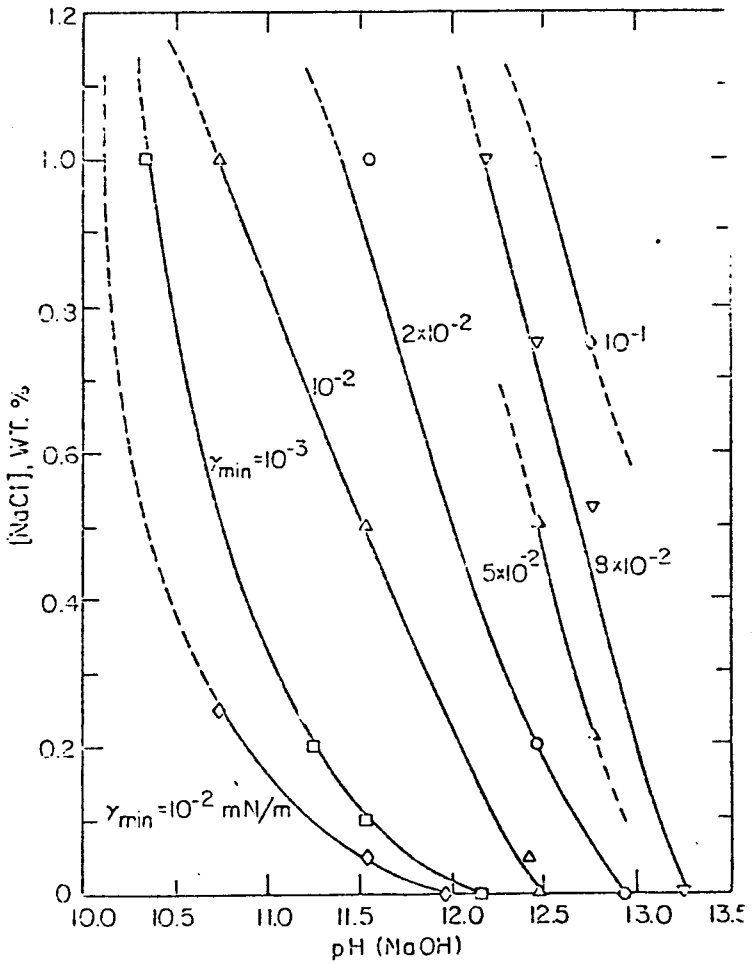

Figure 11 Constant dynamic minimum tensions for varying pH and salt contents.

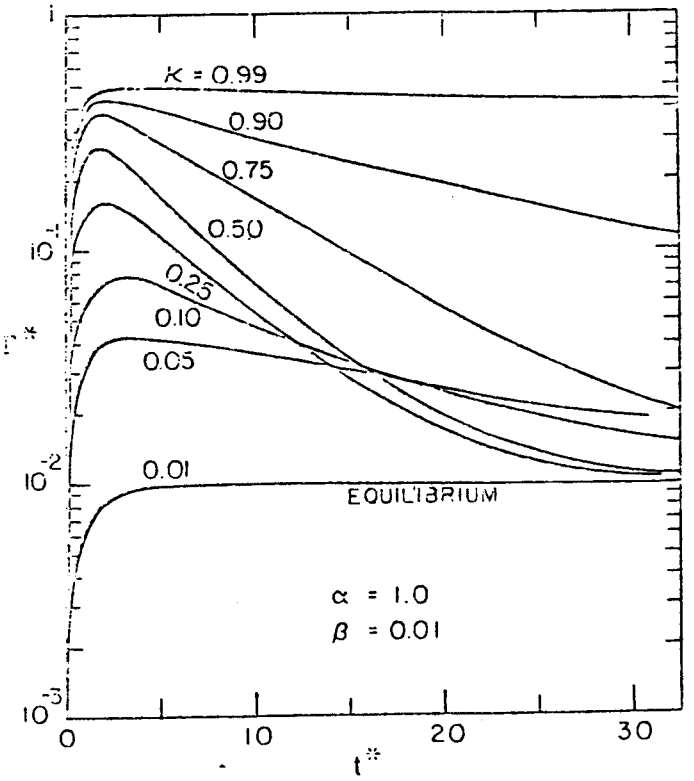

Figure 12. Reduced surfactant adsorption at the oil-water interface versus reduced time. Large κ orresponds to a large desorption barrier into the aqueous phase.

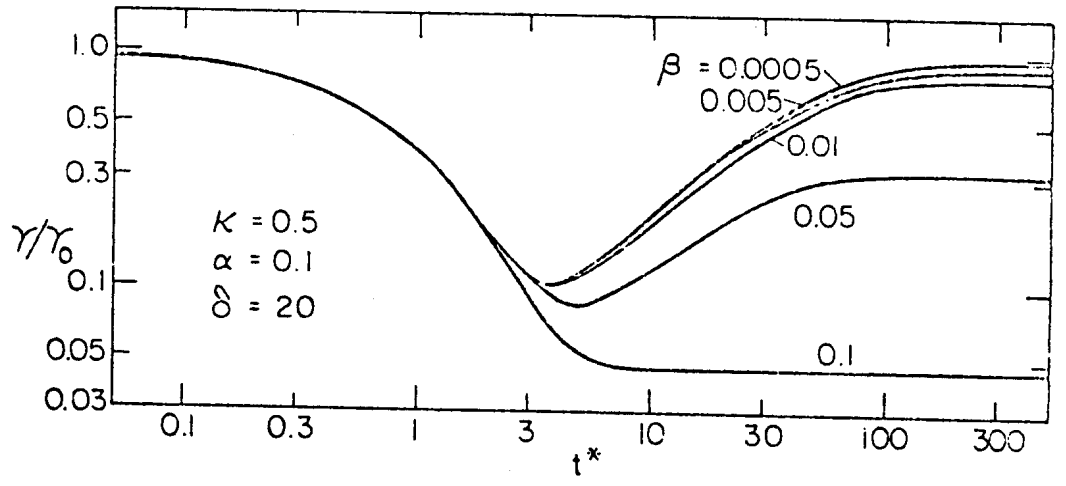

Figure 13. Reduced interfacial tension versus logarithmic reduced time. Decreasing β corresponds to an increasing aqueous volume for a fixed oil drop size.

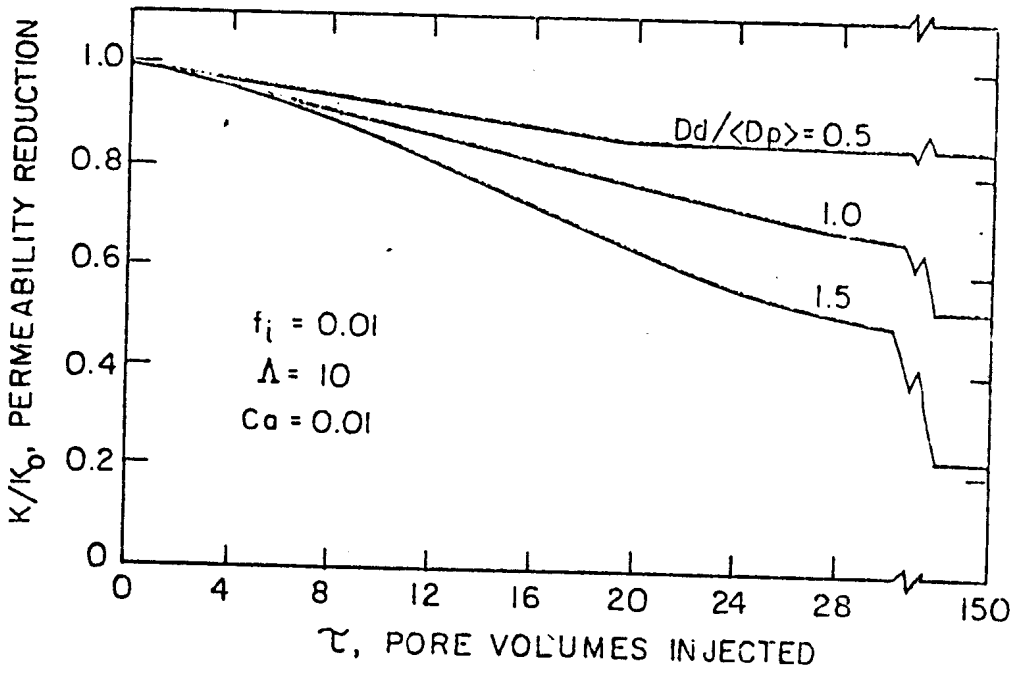

Figure 14. Permeability reduction due to emulsion flow at varying Capillary numbers.